Ecosystems (1998) 1: 268–282

ECOSYSTEMS

Analysis of Large-Scale Spatial Heterogeneity in Vegetation Indices among North American Landscapes

Joan L. Riera,[1]* John J. Magnuson,[1] John R. Vande Castle,[2] and Mark D. MacKenzie[3]

[1]Center for Limnology, Madison, Wisconsin 53706; [2]College of Forest Resources, University of Washington, Seattle, Washington 98195; and [3]School of Forestry, Auburn University, Alabama 36849, USA

ABSTRACT

We analyzed the spatial heterogeneity in vegetation indices among 13 North American landscapes by using full Landsat Thematic Mapper images. Landscapes varied broadly in the statistical distribution of vegetation indices, but were successfully ordinated by using a measure of central tendency (the mean) and a measure of dispersion (the standard deviation or the coefficient of variation). Differences in heterogeneity among landscapes were explained by their topographic relief and their land cover. Landscape heterogeneity (standard deviation of the Normalized Difference Vegetation Index, NDVI) tended to increase linearly with topographic relief (standard deviation of elevation), but landscapes with low relief were much more heterogeneous than expected from this relationship. The latter were characterized by a large proportion of agricultural land. Percent agriculture, in turn, was inversely related to topographic relief. The strength of these relationships was evaluated against changes in image spatial resolution (grain size). Aggregation of NDVI images to coarser grain size resulted in steady decline of their standard deviation. Although the relationship between landscape heterogeneity and explanatory variables was generally preserved, rates of decrease in heterogeneity with grain size differed among landscapes. A spatial autocorrelation analysis showed that rates of decrease were related to the scale at which pattern is manifested. On one end of the spectrum are agricultural, low-relief landscapes with low spatial autocorrelation and small-scale heterogeneity associated with fields; their heterogeneity decreased sharply as grain size increased. At the other end, desert landscapes were characterized by low small-scale heterogeneity, high spatial autocorrelation, and almost no change in heterogeneity as grain sized was increased—their heterogeneity, associated with land forms, was present at a large scale.

Key words: landscapes, spatial heterogeneity, vegetation indices, Landsat TM, AVHRR, scale, topography, land use.

INTRODUCTION

Despite early recognition by ecologists that spatial heterogeneity is important for understanding ecological processes (McIntosh 1991), spatial variability, and the issues associated with spatial scaling, have been traditionally neglected (Magnuson and others 1991; Levin 1992; Kareiva 1994; Kratz and others 1995). Yet the environmental problems that face us (global change, land-use change, landscape fragmentation, and loss of biodiversity) require that ecologists deal with structures and processes at regional to global scales and across heterogeneous and changing landscape mosaics (Turner and others 1995). Landscape ecology expands the scope of ecology to address the role of spatial heterogeneity in ecological processes (Picket and Cadenasso 1995).

Spatial heterogeneity is an important property of landscapes (Kolasa and Picket 1991; Li and Reynolds 1995). On the one hand, it reflects the operation of processes and constraints responsible for the generation of pattern (Urban and others

Received 1 October 1997; accepted 11 February 1998.
*Corresponding author. e-mail: jlrey@facstaff.wise.edu

1987). On the other hand, landscape heterogeneity affects many ecological processes. To understand how those processes operate, it is essential to characterize spatial heterogeneity (Turner 1989a, 1989b).

Spatial heterogeneity is manifested at different scales, determined by the pattern-generating processes (Urban and others 1987; Picket and Cadenasso 1995). For example, at a small scale (small extent, small grain, short temporal resolution), spatial heterogeneity in vegetation can be related to microenvironments, species dispersal, or competition processes. At a medium scale, it can be related to disturbances such as windthrow or fires. At a larger scale, topography and climate may be overriding constraints (Urban and others 1987).

The ability to detect and explain spatial heterogeneity depends on the scale of observation. At a large scale (regional, to continental, to global), remote sensing provides the only means to collect synoptic data with high spatial resolution (Quatrocchi and Pelletier 1991; Roughgarden and others 1991). Spectral vegetation indices, which exploit differences in green vegetation in absorption of red radiation and reflectance of near-infrared radiation, provide a surrogate for vegetation properties such as cover, above-ground biomass, leaf-area index, or absorbed photosynthetically active radiation (Tucker and Seller 1986; Baret and Guyot 1991; Myneni and others 1995).

To investigate the role of heterogeneity in structure and function at larger spatial scales than traditionally analyzed by ecologists, it is first necessary to observe this heterogeneity quantitatively and determine its major determinants. Our goal is to measure large-scale heterogeneity in vegetation, compare these measures among disparate landscapes, and explain the observed patterns through explanatory variables and the influence of changing scales of observation. The landscapes we studied comprise a wide range of North American biomes, from boreal forest in Alaska to hot desert in New Mexico. We used entire Landsat Thematic Mapper (TM) images and two of the most widely used vegetation indices: the simple ratio vegetation index (SR), and the Normalized Difference Vegetation Index (NDVI).

At a continental scale, mean vegetation cover and biomass are constrained by climate and elevation [that is, by the magnitude and variance of solar radiation and water availability (Schlesinger 1991)]. We hypothesized that at the extent of full Landsat TM images, variability in vegetation cover and biomass, and hence heterogeneity in vegetation indices, would be related to topographic relief and to land use/land cover. Land modification by humans is a powerful force shaping landscapes at a regional to global scale (Meyer and Turner 1994).

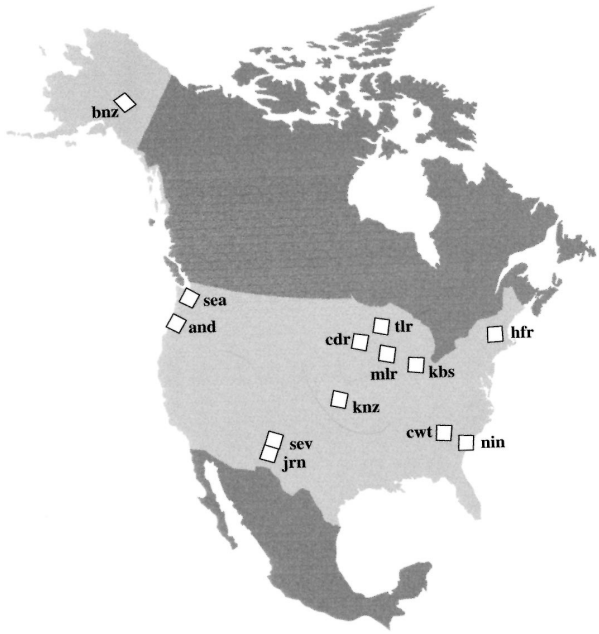

Figure 1. Location of landscapes in North America. Polygons correspond to extent of Landsat Thematic Mapper images. See Table 1 for explanation of abbreviations.

Our specific objectives are (1) to characterize landscapes by the heterogeneity in their vegetation indices, (2) to select an appropriate metric for the comparison of heterogeneity across landscapes, (3) to ordinate landscapes based on that metric, (4) to assess the contribution of surface water and of ice plus snow to landscape heterogeneity, (5) to relate heterogeneity in vegetation to topography and land use, and (6) to assess the effects of changing grain size on heterogeneity.

Data Sources and Methods

Study Landscapes

We compared 13 sites located across the conterminous United States and in Alaska (Figure 1). The landscapes comprised a wide range of biomes (Table 1), including boreal forest (BNZ), temperate rain forest (SEA), temperate coniferous (AND) and deciduous (CDR, CWT, and HFR) forest, grassland (KNZ), and desert (JRN and SEV). Moreover, two of the scenes were dominated by agricultural landscapes (KBS and MLR). The proportion of inland water bodies in the scenes varied greatly, with its maximum representation in Northern Wisconsin (TLR) and the Seattle area (SEA). In one of the

Table 1. Satellite Images Used in This Study

Acronym	LTER Site in the Scene	Vegetation Type at LTER Site	Row/Path	Acquisition Date
AND	H. J. Andrews Experimental Forest	Temperate coniferous forest	46/29	7 July 1991
BNZ	Bonanza Creek Experimental Forest	Boreal forest	69/15	22 June 1991
CDR	Cedar Creek Natural History Area	Eastern deciduous forest and tall-grass prairie	27/29	18 July 1991
CWT	Coweeta Hydrologic Laboratory	Eastern deciduous forest	18/36	3 July 1991
HFR	Harvard Forest	Eastern deciduous forest	13/30	16 July 1991
JRN	Jornada Experimental Range	Hot desert and mesquite dunes	33/37	26 July 1991
KBS	Kellogg Biological Station	Agricultural landscape	21/31	6 June 1991
KNZ	Konza Prairie	Tall-grass prairie	28/33	26 August 1991
MLR	Madison Lake Region[a]	Agricultural landscape	24/30	10 July 1989
NIN	North Inlet Marsh	Estuary, marshes, eastern deciduous forest	16/37	2 May 1991
SEA	Seattle Area	Temperate rain forest, high mountain	46/27	7 July 1991
SEV	Sevilleta National Wildlife Refuge	Mixed-conifer forest, grassland, desert	33/36	3 September 1991
TLR	Trout Lake Region[a]	Eastern deciduous forest, wetlands and lakes	25/28	5 August 1991

[a]*MLR and TLR are two regions within the North Temperate Lakes (NTL) Long-Term Ecological Research (LTER) site.*

scenes (BNZ, Alaska), glaciers were a significant component of the landscape.

Satellite Images

We acquired Landsat TM images for each of the study landscapes. Because spatial heterogeneity is scale dependent (Milne 1991), the choice of satellite sensor, and hence of scale, sets the boundaries for the analysis. For our analyses, we chose full Landsat TM images because of its relatively fine grain (approximately 30 m) and large extent (swath, 185 km). Each image contained a site of the Long-Term Ecological Research (LTER) Network (Table 1), except for Cedar Creek (CDR), where the LTER site lies just off the north edge of the image. Scenes were acquired by the LTER Network, with the exception of the Seattle scene (SEA), which was obtained as part of the US Geological Survey Biological Resources Division GAP analysis program (Vande Castle and others 1995). To minimize the influence of interannual and seasonal variability of vegetation cover on our analysis, we limited image acquisition dates to the growing season of 1991, with the exception of the Madison Lakes Region (MLR), which was acquired during the growing season of 1989. Acquisition dates ranged from 2 May to 3 September, with 11 of 13 images in June, July, or August. A closer seasonal grouping was prevented by our choice of images with low cloud cover (less than 10%; the proportion of clouds plus cloud shadows in the landscapes varied from a minimum of 0.1% for NIN to a maximum of 16.5% for BNZ).

The LTER Network has focused on the collection of consistent long-term data at a set of diverse ecosystems across North America (Brenneman 1989; Franklin and others 1990; Magnuson and others 1991). By using imagery containing LTER sites, we assured (a) access and relevance to a growing, maintained database of satellite imagery (currently over 80 images), (b) access to a body of long-term ecological research at the sites, and (c) the potential for contrasting our results with previous comparative analyses among LTER sites (Kratz and others 1995).

Image Classification

Each image was classified to remove clouds and cloud shadows and to discriminate between land, water, and snow plus ice. The classification process, which used all seven bands provided by the Landsat TM sensor, started with an unsupervised classification, followed by an iterative series of supervised classifications. We continued the iterative classification until no net improvement was visually observed. We assigned the numerous classes to land, water, snow + ice, or clouds + shade. The resulting images were then used as masks in the calculation of descriptive statistics for each class. All classifications were done with the image analysis package ERDAS 7.5. Sources of error in the classification

include mixed pixels (for example, at the edge of water bodies), and confused classes when spectral signatures were similar. This was the case for some wetlands (confusion between water and land) and shadows of clouds (occasionally confused with land or water). Portions of the ocean visible in three of the scenes [Andrews (AND), Seattle (SEA), and North Inlet (NIN)] were removed from the analysis.

Vegetation Indices

Two widely used vegetation indices were calculated. Both exploit the differential response of green vegetation with respect to other surfaces to the red (absorbed by vegetation) and near-infrared (reflected by vegetation) portions of the electromagnetic spectrum (EMS). The SR is defined as

$$SR = \frac{TM4}{TM3}$$

and the NDVI as

$$NDVI = \frac{TM4 - TM3}{TM4 + TM3}$$

where TM3 is the reflectance in band 3 (0.63–0.69 μm), which corresponds to the red portion of the EMS; and TM4 is the reflectance in band 4 (0.76–0.90 μm), which corresponds to the near-infrared, of the Landsat TM sensor (Lillesand and Kiefer 1994). Before calculating indices, images were radiometrically corrected to make them comparable by converting digital numbers to radiance and then normalizing them to percent at-sensor reflectance (Vande Castle and others 1995). No attempt was made to correct for atmospheric interference or topographic influence. Ratio-based indices, however, reduce topographic effects on spectral response. Vegetation indices were calculated using custom models written for ERDAS Imagine 8.2, and the results were stored as 32-bit floating-point numbers (Vande Castle and others 1995).

Statistics

Histograms and descriptive statistics (minimum, maximum, mean, median, and standard deviation) were calculated for each vegetation index by class component (that is, land, land plus water, and land plus water plus ice and snow). The coefficient of variation was calculated as the standard deviation divided by the mean.

Skewness and kurtosis were estimated from histograms using SAS (SAS 1988). Histograms were produced using 300 data intervals or bins within the following ranges of values: −1 to +1 for NDVI, and 0 to 30 for SR. The range for NDVI comprises the entire range of values that this index can take on. SR takes on nonnegative values and is unbounded, but because some scenes contained extremely high values, we selected an upper bound (SR = 30) that was assigned to all pixels exceeding that value. The number of pixels in this category was negligible in all scenes. The number of bins per histogram (300) was chosen to be in the same order of magnitude as the radiometric resolution of the original data (that is, 8 bits). Given the large number of pixels per scene, this decision did not affect our results. Statistics calculated on the full scene and estimated from 300-bin histograms and from 100-bin histograms were similar (data not shown).

Explanatory Variables

As a measure of topographic relief, we used the standard deviation of elevation. Elevation was derived from the 30 arc-second Digital Chart of the World (DCW) Digital Elevation Model (DEM) (Defense Mapping Agency 1992). This is a moderate resolution topographic data set, with pixel resolutions of 30 arc-seconds (approximately 1 × 1 km, but varying with latitude). [The absolute reported accuracy of the vector contour data from which this digital elevation model was derived is 2000 m circular error (horizontal) and ±650 m linear error (vertical) at 90% confidence interval (Defense Mapping Agency 1992). The accuracy for the grid has not been measured or calculated, but will not be more accurate than its source.]

Land use/land cover was obtained at a similar spatial resolution from the Conterminous US Land Cover Characteristics Data Set 1990 prototype (Loveland and others 1991), which was acquired through the Socioeconomic Data and Applications Center (SEDAC; URL, http://sedac.ciesin.org). This is a classification of seasonal land-cover types at 1-km resolution. The data set was produced by the US Geological Survey EROS Data Center and the Center for Advanced Land Management Information Technologies at the University of Nebraska–Lincoln. Original data for the classification were from National Oceanic and Atmospheric Administration's Advanced Very High Resolution Radiometer (AVHRR) satellite imagery. The information derived from satellite images was combined with ancillary earth science data sets (such as climate, elevation, and ecoregions) to produce a classification of land cover comprising 159 distinct classes.

We merged the original classes into seven broad categories: agricultural land (mostly irrigated), forage/rangeland/pasture, forest, marsh, barren and urban, alpine tundra, and open water (Table 2). The first three categories comprised over 95% of the

Table 2. Aggregated Land-Cover Classes

Land-Cover Class (This Study)	Land-Cover Key in Land-Cover Characteristics Prototype
Agriculture	1–54
Forage/rangeland/pasture	55–86
Forest	87–148
Water	149
Wetlands	150–154
Urban and barren	155
Alpine tundra	156–159

Socioeconomic Data and Applications Center: URL, http://sedac.ciesin.org.

land area in each landscape studied (Table 3). The proportions of each of these three major classes were used as explanatory variables. Land-cover data were not available for Bonanza, Alaska (BNZ).

Multiscale Analysis

Measures of spatial heterogeneity often depend on the scale of observation (Milne 1991; O'Neill and others 1991). Therefore, it is important to evaluate how heterogeneity changes with grain size. In our study, an additional complication was that statistics were calculated at the native scale of each data set. When measures of heterogeneity were related to explanatory variables, a mismatch in scale occurred. While extent was preserved across data sets, grain size was approximately 30 m for Landsat TM, but about 1 km for elevation and land cover.

We used two different approaches to explore the relationship between heterogeneity and grain. The first was to aggregate Landsat NDVI images to progressively coarser spatial resolutions and then recalculate image statistics at each new scale. Image pixel aggregation was accomplished by averaging pixel values using nonoverlapping windows. Window size was varied from 2×2 (that is, 60×60 m) to 100×100 (that is, 3×3 km) by adding one row and one column to the averaging window at each iteration. NDVI images were masked so that only land values were used in calculations, because we wanted to avoid an increase in land heterogeneity owing to contamination of land pixels with other classes. Aggregating NDVI images rather than aggregating the original reflectance bands and then recalculating NDVI at each scale probably did not affect the results at the scales of our analysis (Aman and others 1992; De Cola 1997).

The second approach was to calculate NDVI statistics from the conterminous US 1-km AVHRR data collected and composited biweekly during 1991 by the EROS Data Center. Biweekly composites are created by first selecting all images with low cloud cover, calculating NDVI, and then selecting, for each given pixel, the highest NDVI value recorded (Eidenshink 1992). For each landscape, we used the biweekly composite that included the corresponding acquisition date for the Landsat TM images (Table 1). Because AVHRR composites are not available before 1991, the Madison Lakes Region (MLR) site had to be excluded from this analysis. Because we were interested in land heterogeneity, we masked water and ice plus snow in the AVHRR images by using a threshold value of NDVI ≤ 0.09 (Loveland and others 1991), except for the two desert landscapes (NDVI ≤ 0.13), where a low threshold would have excluded large, sparsely vegetated areas from the analysis. Vegetation heterogeneity was calculated as the standard deviation of NDVI, and values were compared with those obtained from Landsat scenes aggregated to 1020-m pixel size.

Spatial Autocorrelation

A neutral landscape constructed by randomly assigning values for NDVI to each pixel to ensure the lack of spatial autocorrelation would respond to an aggregation of pixels by decreasing its variance (or standard deviation) according to the proportionality

$$\ln S^2 \approx a - \ln n$$

where S^2 is the sample variance, a is a proportionality constant, and n is the sample unit size (that is, pixel size), which in our aggregation procedure increases as the number of samples (that is, number of pixels) decreases. The slope of this linear relationship is -1.

If NDVI values, however, were not spatially independent, then the slope of this relationship would vary between -1 and 0 [see O'Neill and others (1991) and references therein]. Since any natural landscape is expected to show spatial autocorrelation to some degree, our landscapes should present slopes closer to zero, with differences in slope related to differences in spatial autocorrelation among landscapes.

We hypothesize that differences in slope (that is, in the rate of variance decrease as grain size increases) among landscape will be not be related to their heterogeneity at the original scale of Landsat TM images (that is, approximately 30-m grain size), but to their degree of spatial autocorrelation at that scale, that is, to the configuration of landscape pattern.

To test this hypothesis, we calculated slopes of the log–log relationship between variance and grain size for each landscape, and plotted them against a

Table 3. Proportion of Land-Cover Classes Per Landscape

Land-Cover Class	JRN	SEV	CWT	SEA	AND	TLR	HFR	NIN	KNZ	MLR	CDR	KBS
Agriculture	0.55	2.37	7.97	9.10	9.75	12.41	26.23	47.97	61.04	82.42	89.12	94.20
Forage/rangeland/pasture	80.67	89.74	0.05	1.19	0.13	0.01	0.01	0.65	34.03	0.09	0.22	0.01
Forest	15.94	7.89	90.73	78.35	87.52	84.39	72.57	39.65	4.05	16.72	10.10	4.83
Water	0.31	0.00	1.23	10.41	2.59	3.20	1.19	9.81	0.88	0.78	0.55	0.96
Other	2.52	0.00	0.01	0.95	0.01	0.00	0.00	1.92	0.00	0.00	0.00	0.00

See Table 1 for explanation of the abbreviations. Other includes wetlands, urban and barren, and alpine tundra. Land-cover from the 1991 U.S. Conterminous Land Cover Prototype (Loveland and others, 1991).

simple measure of spatial autocorrelation, Moran's I index (Qi and Wu 1996). This statistic measures the similarity among adjacent pixels, which, in the case of a lattice data set, are defined as the four immediate neighbors of each pixel. Moran's index takes on values between −1 and 1, with 0 values denoting spatial independence, a value of 1 denoting perfect spatial autocorrelation (that is, total homogeneity), and a value of −1 indicating a checkerboard pattern (Cressie 1993). We chose to calculate Moran's index on Landsat TM-derived NDVI images aggregated to a pixel size of 1020 m to ease computational burden and because this pixel size is commensurate with the size of agricultural fields, which we expect to be the major source of heterogeneity at a small scale (small grain size) in our landscapes.

Results

Frequency Distributions of Land Only

Examples of land NDVI frequency distributions in Figure 2 have been ordered along an axis of mean NDVI; a similar ordering could have been done for SR. Mean NDVI values varied from 0.25 to 0.76; mean SR values ranged from 1.7 to 7.8. For both indices, minimum values were at Sevilleta (SEV; desert landscape), and maximum values at Trout Lake Region (TLR; deciduous forest). When only the land component of the scenes was considered, most histograms were unimodal. Some landscapes, however, were bimodal. This was the case for Kellogg Biological Station (KBS; modes at 0.20 and 0.80 NDVI) and for Konza Prairie (KNZ; modes at 0.20 and 0.35 NDVI). Similar patterns were observed for SR distributions.

The relationships among the mean, the standard deviation, and the coefficient of variation among sites differed between NDVI and SR (Figure 3). For NDVI, the standard deviation increased with the mean until it reached a maximum at intermediate values (around 0.5) and then decreased. The coefficient of variation, in contrast, was consistently high for images with mean NDVI below approximately 0.55 and

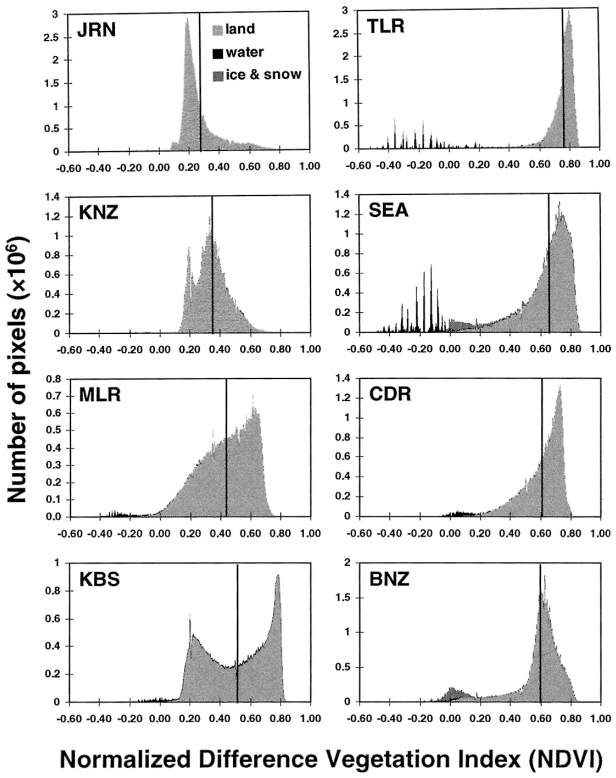

Figure 2. Histograms of normalized difference vegetation index (NDVI) for selected Landsat Thematic Mapper images. Histograms are ordered from lower to higher mean NDVI (vertical line) starting at the top left panel and moving counterclockwise.

then decreased as mean NDVI increased. For SR, the standard deviation increased with the mean and leveled off at about SR = 5, but the coefficient of variation varied with mean SR in the same way that the standard deviation of NDVI did with mean NDVI.

Kurtosis and skewness among sites varied in a regular fashion with mean vegetation index (Figures 2 and 4). Skewness (a measure of the asymmetry of a frequency distribution about its mean) decreased with the mean. It was positive for images with the lowest mean vegetation index, and nega-

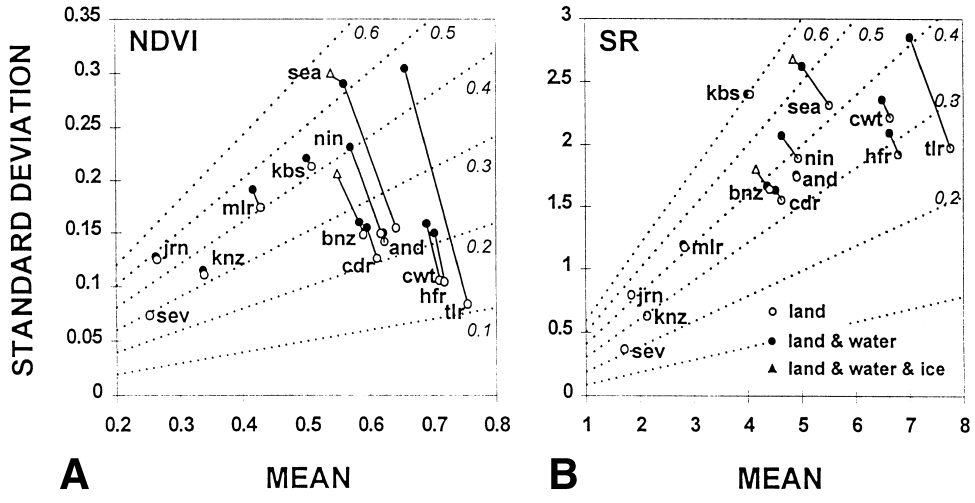

Figure 3. Relationship between the standard deviation and the mean for **A** the normalized difference vegetation index (NDVI) and **B** the simple ratio vegetation index (SR) for full Landsat Thematic Mapper scenes at 30-m grain size. Dotted lines correspond to the coefficient of variation. Solid lines connect values for land, land plus water, and land plus water plus ice and snow, for each of the landscapes.

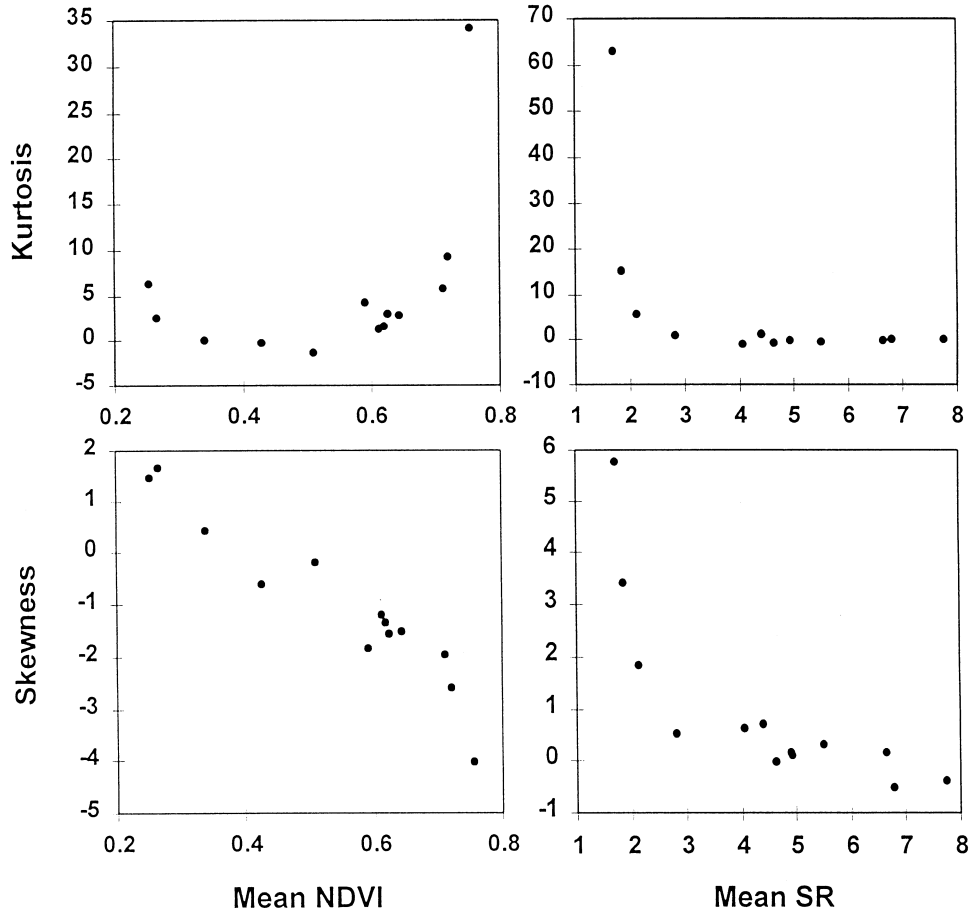

Figure 4. Plots of kurtosis (top panels) and skewness (bottom panels) against mean normalized difference vegetation index (NDVI) (left panels) and mean simple ratio vegetation index (SR) (right panels). Solid lines connect values for land, land plus water, and land plus water plus ice and snow, for each of the landscapes. Data are for full Landsat Thematic Mapper scenes at 30-m grain size.

tive for images with higher mean vegetation index. This negative relationship was linear for NDVI and negative exponential for SR (Figure 4). Kurtosis (a measure of the shape of the distribution about the mean) also varied regularly with the mean. For NDVI, distributions were leptokurtic (that is, tall and narrow) for both sparsely vegetated and profusely vegetated sites, but were brachykurtic (that is, short and wide) for sites with medium mean NDVI. For SR, kurtosis decreased exponentially with mean SR (Figure 4).

Water and Ice Plus Snow

Water, ice, and snow have vegetation index values near zero because, in contrast to vegetation, they neither absorb light in the red portion of the EMS nor reflect differentially in the infrared region. Vegetation index values for water are particularly

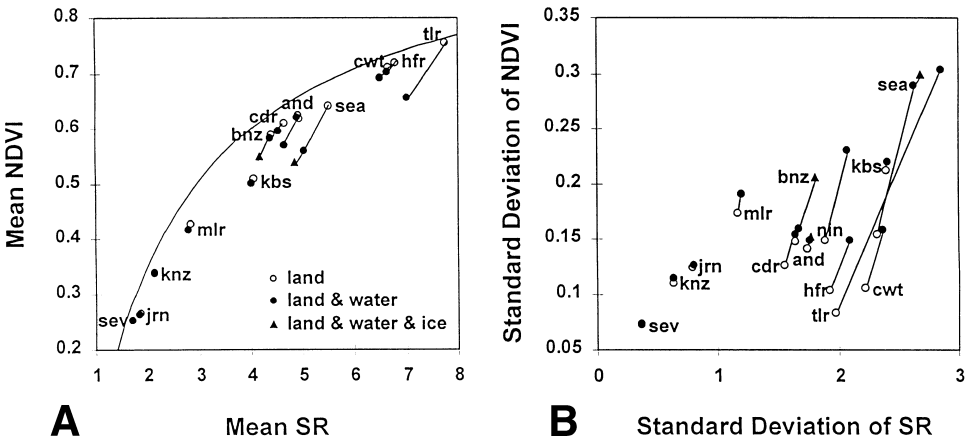

Figure 5. Comparison of normalized difference vegetation index (NDVI) and simple ratio vegetation index (SR): **A** plot of mean NDVI against mean SR, where the solid line is the analytical expression of NDVI against SR; and **B** plot of the standard deviation of NDVI against that of SR. Data are for full Landsat Thematic Mapper scenes at 30-m grain size.

low because water strongly absorbs infrared radiation (Lillesand and Kiefer 1994). This is apparent in the histograms for Seattle Area (SEA) and Trout Lake Region (TLR) in Figure 2. Values of NDVI for water appear disjointed in those histograms probably because the radiometric resolution of the Landsat TM sensor is low at the range of radiation energy reflected by water. Distinct signatures for water of different trophic state, transparency, or water color might contribute to this pattern as well. This disjointed appearance is not perceptible in histograms of SR because this index aggregates low values and spreads large values of the vegetation index.

Where water or ice plus snow are a large component of the landscape, their effect on the statistics describing the frequency distributions of vegetation indices are (a) to lower the mean vegetation index, (b) to increase its standard deviation, and (c) to increase its coefficient of variation (Figure 3). Skewness generally decreases [although it increases in the case of Trout Lake Region (TLR)], whereas the response of kurtosis shows no regular pattern.

SR Compared with NDVI

SR and NDVI are two functionally equivalent vegetation indices that differ in their statistical properties (Perry and Lautenschlager 1984). SR takes on nonnegative values and is unbounded. Its frequency distribution tends to be skewed to the right; its values can be high. In contrast, NDVI is rescaled to be bounded between -1 and $+1$. Its frequency distribution is less skewed; more weight is given to low values. SR and NDVI are analytically related by the expression:

$$\text{NDVI} = \frac{(\text{SR} - 1)}{(\text{SR} + 1)}$$

Sample statistics for each vegetation index, however, cannot be analytically derived from the other.

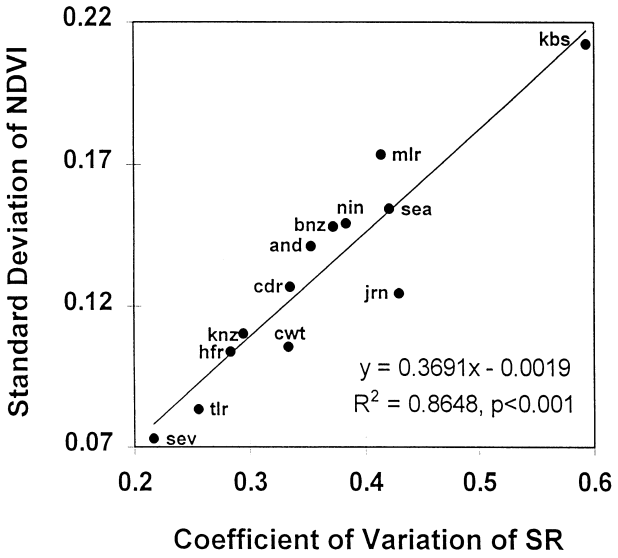

Figure 6. Plot of standard deviation of normalized difference vegetation index (NDVI) against the coefficient of variation of simple ratio vegetation index (SR). The line is a least-squares simple regression.

Ordinations of landscapes with SR and NDVI were similar for means, but differed widely for standard deviation and coefficient of variation, especially if water + ice pixels were excluded (Figure 5). However, the standard deviation of NDVI and the coefficient of variation of SR were linearly related (Figure 6), with a correlation coefficient of 0.93 ($P < 0.001$). The coefficient of variation normalizes the standard deviation by the mean and has a scaling effect equivalent to the normalization performed during the calculation of NDVI. Therefore, the mean and standard deviation of NDVI, and the mean and coefficient of variation of SR, are equivalent for the purposes of this study. Because of its statistical properties (less skewed distribution), we selected

NDVI as a measure of greenness, and its standard deviation as a measure of spatial heterogeneity.

Topography and Land Use

Visual inspection of scatterplots reveals strong relationships between landscape heterogeneity (standard deviation of NDVI) and two explanatory variables: topographic relief (as measured by the standard deviation of elevation) and percent agricultural land (Figure 7A and B).

The relationship between heterogeneity and topography is complex. For landscapes with greater relief [SD(elevation) $>$ 100], NDVI heterogeneity increased linearly with the standard deviation of elevation [SD(NDVI) = 0.0002(elevation) + 0.0646, $n = 8$, $r^2 = 0.82$, $P < 0.002$). Low-relief landscapes [SD(elevation) $<$ 100), contrary to what the previous relationship would suggest, showed the highest heterogeneity. Land cover explains this pattern. Heterogeneity increases linearly with percent agricultural land (Figure 7B). Moreover, percent agricultural land is strongly linked to topographic relief (Figure 7C). In conclusion, landscape heterogeneity appears to be directly related to both topographic relief and percent agricultural land, whereas the latter is inversely related to topographic relief.

Using stepwise multiple-regression analysis, the following model is selected:

$$\text{SD(NDVI)} = 0.05579 + 0.000142\ \text{SD(elevation)} + 0.001228\ \%\text{AGRICULTURE}$$

($n = 12$, RMSE = 0.026, $r^2 = 0.63$, Adj$r^2 = 0.55$, $P < 0.05$)

Other models, including interaction terms or variable transformations to stabilize the variance, do not result in substantial improvements in explanatory power as measured by root mean square error and adjusted r^2. The model with highest statistical significance and highest explanatory power that we obtained was

$$\text{SD(NDVI)} = 0.01888 + 0.13782\ \text{ARCAGRI} + 0.00034\ \text{SD(elevation)} - 0.00063\ \text{INT};$$

(n = 12, RMSE = 0.024, $r^2 = 0.72$, Adj$r^2 = 0.62$, $P < 0.05$)

where ARCAGRI is the arc sine of the square root of percent agricultural land [a common transformation for percentage variables (Draper and Smith

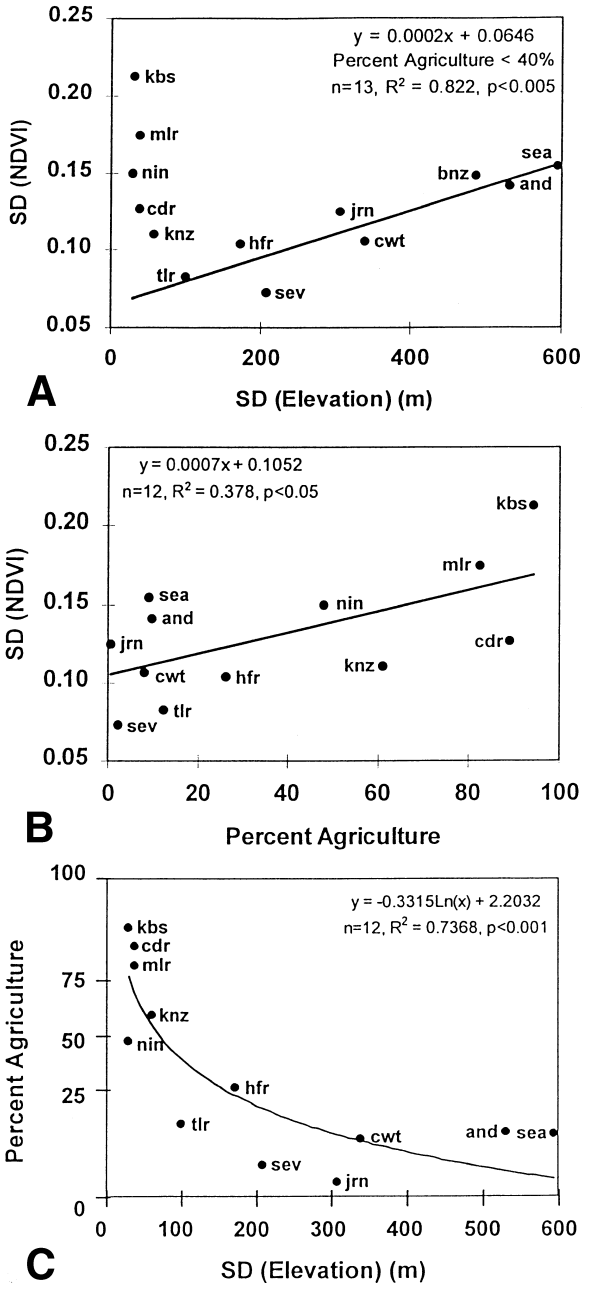

Figure 7. Relationships between landscape heterogeneity and explanatory variables. A Relationship between a measure of landscape heterogeneity (standard deviation of the normalized difference vegetation index, NDVI) and a measure of topographic relief (standard deviation of elevation). The regression equation is for landscapes with less than 40% agricultural land cover. B Relationship between the standard deviation of NDVI and percent agricultural land. The linear regression equation applies to all landscapes. C Relationship between percent cover by agriculture and topographic relief (standard deviation of elevation). Percent agriculture is shown on a transformed axis (arc sine of square root). The model is an exponential equation.

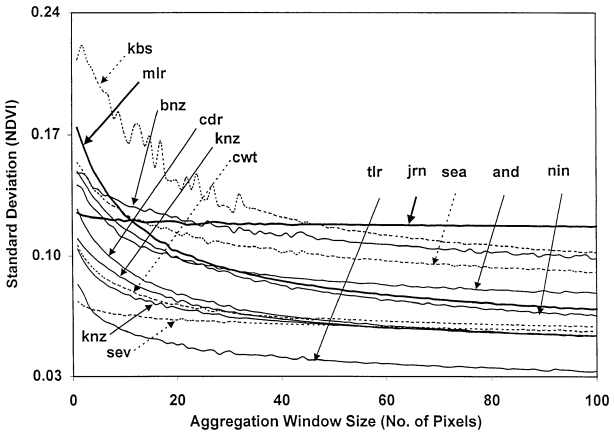

Figure 8. Changes in standard deviation of the land normalized difference vegetation index (NDVI) of full Landsat Thematic Mapper images with grain size. The original grain size (window size of 1 × 1 pixels) is approximately 30 × 30 m. The coarsest grain size analyzed is 100 × 100 pixels, or approximately 3 × 3 km.

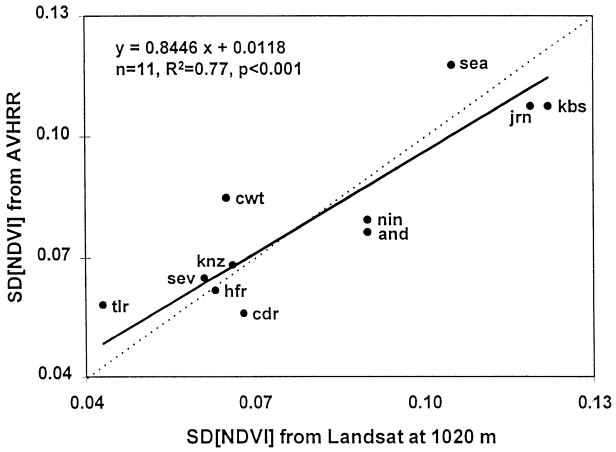

Figure 9. Comparison between the standard deviation of the normalized difference vegetation index (NDVI) from Advanced Very High Resolution (AVHRR) images (pixel size, approximately 1000 m) and from aggregated Landsat images (pixel size, about 1020 m). The solid line is a geometric regression line, and the broken line is the one-to-one relationship.

1981)], and INT is the interaction term between the two independent variables.

Multiscale Analysis

As expected, the standard deviation of NDVI decreased as grain size increased (closely following a negative exponential curve) because, as pixel size increases, pixel values tend to converge to the image mean value. But the rate at which the standard deviation of NDVI decreased varied markedly among landscapes (Figure 8). The fastest decrease rate was found at the southern Wisconsin site (MLR), where the standard deviation of NDVI went from 0.17 at 30-m resolution to 0.065 at 3-km resolution. The slowest decrease rates were observed at the two desert sites (JRN and SEV). The mean and standard deviation of NDVI obtained from AVHRR images (grain size = 1 km) are in general agreement with the same statistics obtained by aggregating Landsat TM images to a grain size of 1020 m (Figure 9). Despite the scatter of points, a geometric linear regression [preferred over simple least-squares because the purpose was not prediction, but description of the relationship (Sokal and Rohlf 1981)] yields a slope close to 1 and an intercept close to 0 (Figure 9). The scatter may result from using composite images, from differences in the field of view of the two sensors, or from contamination of land pixels with water and ice plus snow in the AVHRR images.

Autocorrelation Analysis

The rate at which heterogeneity decreased with increasing pixel size was related strongly to small

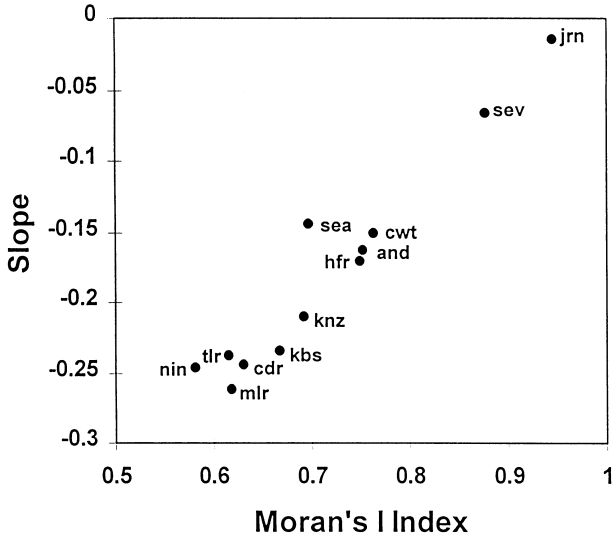

Figure 10. The slope of the logarithm of the standard deviation of the normalized difference vegetation index versus the logarithm of pixel size, plotted against Moran's I index, a measure of spatial autocorrelation.

scale (1-km grain size) spatial autocorrelation (Figure 10). All the landscapes with low relief have low values of Moran's I index (that is, low spatial autocorrelation), indicating that the observed heterogeneity is manifested at a small scale. In five of these landscapes (NIN, MLR, CDR, and KBS), the heterogeneity is associated with agriculture. In accordance with their low spatial autocorrelation, these landscapes present the lowest slopes (closer to −1), indicating that the standard deviation of NDVI

decreases rapidly as grain size is increased. In contrast, desert landscapes, whose heterogeneity decreases only slightly throughout the range of pixel sizes analyzed, have high spatial autocorrelation at the scale of 1 km.

DISCUSSION

Comparison of Heterogeneity Among Landscapes

Landscape ecology is concerned with the detection, measurement, and interpretation of pattern, the relationship between pattern and ecological processes, and the dependency of pattern and process on spatial scale (Forman and Godron 1986; Turner 1989a). Our study addresses these aspects through a comparison of landscape heterogeneity among North American landscapes. We detect and measure heterogeneity in spectral vegetation indices, ordinate these landscapes according to the statistical properties of those indices, relate heterogeneity across landscapes to two explanatory variables (topography and land use), and explore the dependency of those relationships on scale (grain size).

The landscapes showed a rich array of pattern in spectral vegetation indices, yet only two statistics were needed to ordinate them: a measure of central tendency and a measure of dispersion. We selected the mean and standard deviation of NDVI as statistics, but other combinations would have been possible, as long as care were taken to normalize the variability in the vegetation index to the magnitude of the index. In the case of NDVI, such normalization is performed by the index itself. If SR is used, the coefficient of variation should be used as a measure of heterogeneity.

At the native scale of Landsat TM images (pixel size $\approx$30 m), land spatial heterogeneity was greatest for landscapes with intermediate mean vegetation indices, such as Kellogg Biological Station (KBS) and Madison Lakes Region (MLR). Desert landscapes (JRN and SEV) and grassland landscapes (KNZ) had low mean NDVI and low overall heterogeneity, whereas landscapes dominated by forest (for example, CWT, HFR, and TLR) had high mean vegetation indices, but low heterogeneity. This relation is altered when other landscape components (water, ice, and snow) are included. These components are more common in wetter landscapes, where mean vegetation indices are high. Spatial heterogeneity of those landscapes is increased by inclusion of water and ice plus snow, which are well-defined patches with low vegetation index values.

Other studies have reported marked differences in spatial heterogeneity across landscapes by using satellite imagery. Landsat TM radiance and radiance coefficient of variation were useful in discriminating cover types in the seasonal tropics (Rey-Benayas and Pope 1995). Musick and Grover (1991) used textural measures to compare satellite images of diverse landscapes. An important difference is that their measures implicitly incorporate the scale and spatial distribution of pixel values. Our measures of overall spatial heterogeneity, however, are insensitive to how vegetation index values are distributed across the images.

Spatial configuration is an important characteristic of pattern (Li and Reynolds 1995). The values we have obtained for overall spatial heterogeneity can result from different spatial configurations. In particular, a similar value can be obtained with a few large patches of homogeneous vegetation index values (that is, large-scale heterogeneity) or with many small, scattered patches of dissimilar values (that is, small-scale heterogeneity). More commonly, a combination of large-scale and small-scale heterogeneity will be found, with heterogeneity manifested at nested hierarchical levels (Allen and Hoekstra 1992). We addressed this issue by manipulating the scale of the satellite images and calculating heterogeneity as a function of scale. Because the scale of analysis influences the relationship of heterogeneity to explanatory variables, we first discuss the explanatory variables at a full Landsat scale.

Explanatory Variables

The detection and measurement of observed heterogeneity only acquires ecological significance when the agents of pattern formation can be identified by using independent observations. Spatial pattern in vegetation, and hence in vegetation indices, can be the result of disturbance processes, biotic processes, or environmental constraints (Levin 1978, 1992; Urban and others 1987). The importance of each agent of pattern generation varies with scale. We have hypothesized that, at the scale of North America, topography and land use/land cover would be of overriding importance.

Topography acts as a surrogate for a number of environmental constraints that limit the development of vegetation, such as temperature, water availability, and incident radiation. On a pixel-by-pixel basis, the relationship between NDVI and topography has been established for several landscapes (Bian and Walsh 1993; Bian 1997; Walsh and others 1997). Here we demonstrate a general relationship between the heterogeneity of vegetation and the heterogeneity of elevation across landscapes: as

the complexity of the topography increases, so does the heterogeneity of vegetation as measured by the standard deviation of NDVI (Figure 7a).

This relationship breaks down for landscapes with low relief. This results from the contribution of human land uses, and specifically of agriculture, on the measured heterogeneity of NDVI. Large-scale agricultural developments are restricted to low-relief land. Their disproportionate contribution to NDVI heterogeneity is easily explained, as agricultural areas are mosaics of fields with different crops or at different phenological states. Our results recognize the widespread transformation of the land surface by human activities and emphasize the need to link landscape models to land-use/cover extent and change (Thomas 1956; Turner and others 1990; Meyer and Turner 1994; Vitousek and others 1997).

Is spatial heterogeneity a desirable property of landscapes? Assessing the human value of heterogeneity is an important question for land managers. Yet the answer to this question is nonexistent because the question is not adequately posed. Landscape heterogeneity has been related to biodiversity in tropical forests (Rey-Benayas and Pope 1995), but in our study the most human-dominated landscapes present the highest heterogeneity. Landscape heterogeneity is as vague a term as ecological variability (Kareiva and Bergelson 1997) or biodiversity when viewed in the sense of human values. The meaning of heterogeneity needs to be rendered precise by specifying the data characteristics, scale, method of calculation, and purpose of the study (Li and Reynolds 1995). In our study, heterogeneity only acquires meaning when it is related to explanatory variables (topography and land cover) and when its dependence on scale is assessed. And an additional step is required: Kolasa and Rollo (1991) suggest that measured heterogeneity needs to be turned into functional heterogeneity, that is, heterogeneity from the perspective of participating ecological entities.

Multiscale Analysis

We have compared landscapes according to their spatial heterogeneity at the scale of full Landsat TM scenes and then explained the differences among landscapes in heterogeneity from topography and land use/land cover. To what degree does the order of these landscapes along an axis of heterogeneity change? Does the relationship between spatial heterogeneity with topography and land cover hold at different scales?

Scale has been identified as a central issue in remote sensing and in the Geographic Information System (GIS) (Quatrocchi and Goodchild 1997), in global ecology (Ehleringer and Field 1993), in landscape ecology (Meentemeyer and Box 1987; Turner and others 1989a; Milne 1991), and in ecology generally (Allen and Starr 1982; Levin 1992). The observed pattern and variability of a system are conditional on the scale of description. Relationships established at one scale are not guaranteed to hold at another, because processes or constraints that are significant at one scale may not operate at another. Landscape heterogeneity is a multiscale property of landscapes (Milne 1991; O'Neill and others 1991; Turner and others 1989b)

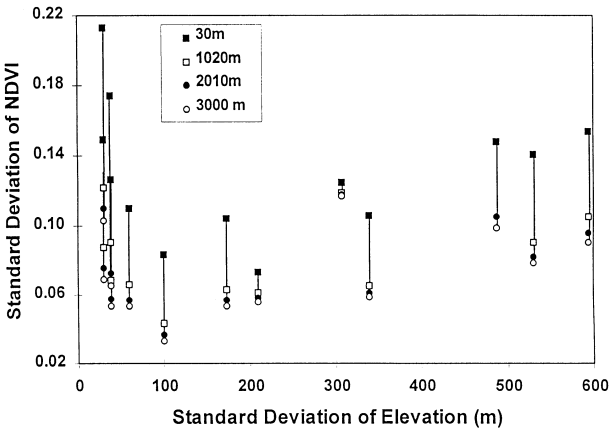

Figure 11. The standard deviation of the normalized difference vegetation index (NDVI) calculated at four grain sizes, from native (approximately 30 m) and aggregated (1020, 2010, and 3000 m) Landsat images, plotted against the standard deviation of elevation (pixel size, approximately 1000 m).

Scale is a concept of broad meaning (Goodchild and Quatrocchi 1997). We took it to comprise the spatial extent, grain (spatial resolution), spectral resolution, and temporal resolution of analysis. Because our data were Landsat TM-derived NDVI images, and because the native scale of our explanatory variables was coarser than the Landsat data, we were particularly concerned with the effect of changes in grain.

Ordering of landscapes according to their spatial heterogeneity changed with the grain size of the image. As expected, the standard deviation of NDVI decreased with grain size, a consequence of the smoothing produced by the aggregation technique (Bian 1997), but it decreased at different rates for different landscapes (Figure 8). An important consequence of the differential decrease of heterogeneity with grain is that its relationship with topography and land cover also changes (Figures 8 and 11). As we coarsened the grain size from 30 m to 3 km, the decrease in heterogeneity was more pronounced for agricultural landscapes than for forested landscapes,

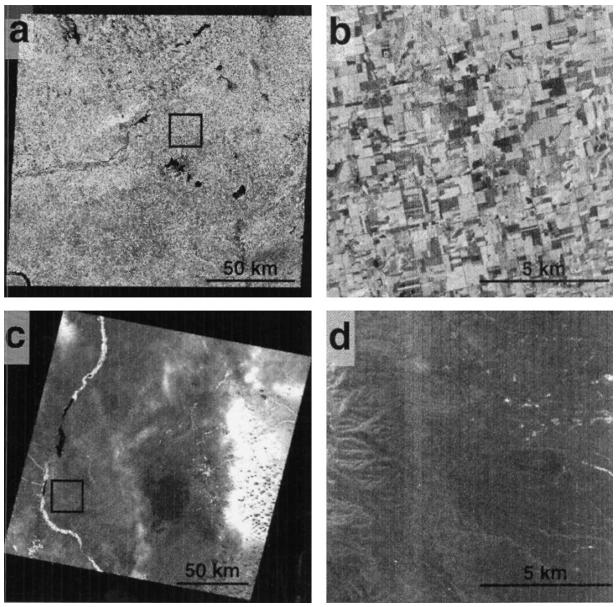

Figure 12. Two contrasting examples of landscapes: a and b the Madison Lakes Region (MLR), an agricultural landscape characterized by low relief and small-scale heterogeneity, and c and d Jornada (JRN), a desert landscape with large-scale heterogeneity associated with topography. The images show the normalized difference vegetation index (NDVI) for full Landsat Thematic Mapper images (a and c), and for subsets at the finest resolution (b and d).

whereas the heterogeneity of the two desert sites remained almost unaltered. Thus, a landscape that ranked as moderately heterogeneous at the 30-m grain size, the Jornada desert (JRN), became the most heterogeneous one at a grain size of 3 km.

Are these results an artifact of the aggregation procedure? A comparison of aggregated images at approximately 1-km pixel size with AVHRR images of equal pixel size (Figure 9) suggests that the method of aggregation was consistent with the use of coarser-grained remote sensors. Despite some expected scatter in the relationship, both methods yielded remarkably similar values of heterogeneity and produced a similar ranking of landscapes. In particular, the heterogeneity of Jornada (JRN) is among the highest in both aggregated Landsat and AVHRR images, whereas this site ranked among the less heterogeneous when Landsat images were used at their native resolution (30-m pixel size).

What determines the rate of decrease in standard deviation? Visual inspection of the landscapes indicates that heterogeneity is manifested at different scales in different landscapes. Two contrasting examples are MLR, a mainly agricultural landscape in southern Wisconsin, and JRN, a desert landscape in southern New Mexico (Figure 12). Heterogeneity in MLR occurs at the scale of field and small forest patches, but with the low-relief, glaciated landscape, no major geomorphological features add heterogeneity at larger scales. In contrast, the desert landscape displays low small-scale heterogeneity but high large-scale heterogeneity compared with other sites. Large areas dominated by arid shrubland appear homogeneous, whereas, at the scale of kilometers, the landscape is dominated by the contrast between the arid lowlands and the forested hills of the Capitan and Sacramento Mountains, each of which is more homogeneous at a smaller scale.

Landscapes with low spatial autocorrelation at the scale of 1 km should display slopes of log(variance) versus log(sample size) closer to -1 than landscapes with high spatial heterogeneity, which should present slopes closer to 0. This hypothesis is validated by the strong relationship between rate of decrease in heterogeneity and spatial correlation (Figure 10). These analyses emphasize the need to complement the measurement of heterogeneity with an evaluation of how that pattern is distributed across space and how heterogeneity is exhibited at various scales. As previously discussed, vegetation in landscapes is subjected to a variety of pattern-generating agents that operate over varied spatial and temporal scales, perhaps structured hierarchically (Allen and Starr 1982; O'Neill and others 1991).

CONCLUSIONS

Our analysis of the heterogeneity of vegetation indices among North America landscapes has identified explanatory variables for the observed pattern, and has detected and explained scale effects at fine to moderate resolutions (30-m to 3-km grain size). The spatial heterogeneity varies greatly among landscapes at the extent of full Landsat images. This heterogeneity is largely explained by geomorphology (topographic complexity), land cover (especially percent agricultural land), and their interaction. Topographic relief directly affects landscape heterogeneity at large scales, but topographic complexity also indirectly affects the distribution and area covered by agricultural lands and thus heterogeneity at small scales. In low-relief landscapes, where we hypothesize that spatial heterogeneity in vegetation indices would be low, agricultural land uses are the major contributor to spatial heterogeneity.

ACKNOWLEDGMENTS

This research was supported by the Long-Term Ecological Research Program of the National Sci-

ence Foundation (NSF) through a grant to the Network Office (DEB9100342A03). J.J.M. was supported by an NSF midcareer fellowship from the Division of Environmental Biology (DEB9103703). J.L.R. was supported by postdoctoral fellowships from the Spanish Ministry of Education and Science, and from the Centre Interdepartamental de Recerca i Innovació Tecnològica (CIRIT) of the Catalan Autonomous Government (1995BEAI300126). We thank the LTER Network Office at the University of Washington and the College of Forest Resources for facilitating the study during J.J.M.'s midcareer fellowship at the University of Washington, Seattle. We thank Randolph Wynne for comments on a earlier draft.

References

Allen TFH, Starr TB. 1982. Hierarchy: perspectives for ecological complexity. Chicago: University of Chicago Press.

Allen TFH, Hoekstra TW. 1992. Toward a unified ecology. New York: Columbia University Press.

Aman A, Randriamanantena HP, Posaire A, Frouin R. 1992. Upscale integration of the normalized difference vegetation index: the problem of spatial heterogeneity. IEEE Trans Geosci Remote Sens 30:326–38.

Baret F, Guyot G. 1991. Potentials and limits of vegetation indices for LAI and APAR assessment. Remote Sens Environ 35: 161–73.

Bian L. 1997. Multiscale nature of spatial data in scaling up environmental models. In: Quatrocchi DA, Goodchild MF, editors. Scale in remote sensing and GIS. Boca Raton (FL): Lewis. p 13–25.

Bian L, Walsh SJ. 1993. Scale dependencies of vegetation and topography in a mountainous environment of Montana. Prof Geogr 45:1–11.

Brenneman J, editor. 1989. Long-term ecological research in the United States: a network of research sites. 5th ed. Seattle (WA): National Science Foundation Long-Term Ecological Research Network Office.

Cressie NAC. 1993. Statistics for spatial data. New York: John Wiley and Sons.

De Cola L. 1997. Multiresolution covariation among Landsat and AVHRR vegetation indices. In: Quatrocchi DA, Goodchild MF, editors. Scale in remote sensing and GIS. Boca Raton (FL): Lewis. p 73–91.

Defense Mapping Agency. 1992. Development of the digital chart of the world. Washington (DC): US Government Printing Office.

Draper NR, Smith H. 1981. Applied regression analysis. 2nd ed. New York: John Wiley and Sons.

Ehleringer JR, Field CB, editors. 1993. Scaling physiological processes: leaf to globe. San Diego (CA): Academic.

Eidenshink JE. 1992. The 1990 conterminous U.S. AVHRR data set. Photogrammetric Eng Remote Sens 58:809–13.

Forman RTT, Godron M. 1986. Landscape ecology. New York: John Wiley and Sons.

Franklin JF, Bledsoe CS, Callaghan JT. 1990. Contributions of the long-term ecological research program. Bioscience 40:509–23.

Goodchild MF, Quatrochi DA. 1997. Introduction: scale, multiscaling, remote sensing, and GIS. In: Quatrocchi DA, Goodchild MF, editors. Scale in remote sensing and GIS. Boca Raton (FL): Lewis. p 1–12.

Kareiva P. 1994. Space: the final frontier for ecological theory. Ecology 75:1.

Kareiva P, Bergelson J. 1997. The nuances of variability: beyond mean square error and platitudes about fluctuating environments. Ecology 78:1299–300.

Kolasa J, Picket STA, editors. 1991. Ecological heterogeneity. New York: Springer-Verlag.

Kolasa J, Rollo CD. 1991. Introduction: the heterogeneity of heterogeneity—a glossary. In: Kolasa J, Picket STA, editors. Ecological heterogeneity. New York: Springer-Verlag. p 1–23.

Kratz TK, Magnuson JJ, Bayley P, Benson BJ, Berish CW, Bledsoe CS, Blood ER, Bowser CJ, Carpenter SR, Cunningham GL, and others. 1995. Temporal and spatial variability as neglected ecosystem properties: lessons learned from 12 North American ecosystems. In: Rapport DJ, Calow P, editors. Evaluating and monitoring the health of large-scale ecosystems. New York: Springer-Verlag. p 359–83.

Levin SA. 1978. Pattern formation in ecological communities. In: Steele JS, editor. Spatial pattern in plankton communities. New York: Plenum. p 433–65.

Levin SA. 1992. The problem of pattern and scale in ecology. Ecology 73:1943–67.

Li H, Reynolds JF. 1995. On definition and quantification of heterogeneity. Oikos 73:280–4.

Lillesand TM, Kiefer RW. 1994. Remote sensing and image interpretation. 3rd ed. New York: John Wiley and Sons.

Loveland TR, Merchant JW, Ohlen DO, Brown JF. 1991. Development of a land-cover characteristics database for the conterminous U.S. Photogrammetric Eng Remote Sens 57:1453–63.

Magnuson JJ, Kratz TK, Frost TM, Bowser CJ, Benson BJ, Nero R. 1991. Expanding the temporal and spatial scales of ecological research and comparison of divergent ecosystems: roles for LTER in the United States. In: Risser PG, editor. Long-term ecological research. Sussex (UK): John Wiley and Sons. p 45–70.

McIntosh RP. 1991. Concept and terminology of homogeneity and heterogeneity. In: Kolasa J, Picket STA, editors. Ecological heterogeneity. New York: Springer-Verlag. p 24–46.

Meentemeyer V, Box EO. 1987. Scale effects in landscape studies. In: Turner MG, editor. Landscape heterogeneity and disturbance. New York: Springer-Verlag. p 15–34.

Meyer WB, Turner II BL, editors. 1994. Changes in land use and land cover: a global perspective. Cambridge: Cambridge University Press.

Milne BT. 1991. Heterogeneity as a multiscale property of landscapes. In: Kolasa J, Picket STA, editors. Ecological heterogeneity. New York: Springer-Verlag. p 69–84.

Musick HB, Grover HD. 1991. Image textural measures as indices of landscape pattern. In: Turner MG, Gardner RH, editors. Quantitative methods in landscape ecology. New York: Springer-Verlag. p 77–105.

Myneni RB, Hall FG, Sellers PJ, Marshak AL. 1995. The interpretation of spectral vegetation indices. IEEE Trans Geosci Remote Sens 33:481–6.

O'Neill RV, Gardner RH, Milne BT, Turner MG, Jackson B. 1991. Heterogeneity and spatial hierarchies. In: Kolasa J, Picket STA, editors. Ecological heterogeneity. New York: Springer-Verlag. p 85–96.

Perry CR Jr, Lautenschlager LF. 1984. Functional equivalence of spectral vegetation indices. Remote Sens Environ 14:169–82.

Picket STA, Cadenasso ML. 1995. Landscape ecology: spatial heterogeneity in ecological systems. Science 269:331–4.

Qi Y, Wu J. 1996. Effects of changing spatial resolution on the results of landscape pattern analysis using spatial autocorrelation indices. Landscape Ecol 11:39–49.

Quatrocchi DA, Goodchild MF, editors. 1997. Scale in remote sensing and GIS. Boca Raton (FL): Lewis.

Quatrocchi DA, Pelletier RE. 1991. Remote sensing for analysis of landscapes: an introduction. In: Turner MG, Gardner RH, editors. Quantitative methods in landscape ecology. New York: Springer-Verlag. p 51–76.

Rey-Benayas JM, Pope KO. 1995. Landscape heterogeneity and diversity patterns in the seasonal tropics from Landsat TM imagery. Ecol Appl 5:386–94.

Roughgarden J, Running SW, Matson PA. 1991. What does remote sensing do for ecology? Ecology 72:1918–22.

SAS. 1988. SAS procedures guide. Release 6.03 edition. Cary (NC): SAS Institute.

Schlesinger WH. 1991. Biogeochemistry: an analysis of global change. San Diego (CA): Academic.

Sokal RR, Rohlf FJ. 1981. Biometry. 2nd ed. New York: Freeman.

Thomas WL Jr, editor. 1956. Man's role in changing the face of the earth. Chicago: University of Chicago Press.

Tucker CJ, Seller PJ. 1986. Satellite remote sensing of primary productivity. Int J Remote Sens 7:1395–416.

Turner BL, Clark WC, Kates RW, Richards JF, Mathews JT, Meyer WB, editors. 1990. The earth as transformed by human action. Cambridge: Cambridge University Press.

Turner MG. 1989a. Landscape ecology: the effect of pattern on process. Annu Rev Ecol Syst 20:171–97.

Turner MG, editor. 1989b. Landscape heterogeneity and disturbance. New York: Springer-Verlag.

Turner MG, Dale VH, Gardner RH. 1989a. Predicting across scales: theory development and testing. Landscape Ecol 3:245–52.

Turner MG, Gardner RH, O'Neill RV. 1995. Ecological dynamics at broad scales: ecosystems and landscapes. Bioscience 45 Suppl:S29–35.

Turner MG, O'Neill RV, Gardner RH, Milne BT. 1989b. Effects of changing the spatial scale on the analysis of landscape pattern. Landscape Ecol 3:153–62.

Urban DL, O'Neill RV, Shugart HH Jr. 1987. Landscape ecology. Bioscience 37:119–27.

Vande Castle JR, Magnuson JJ, MacKenzie MD, Riera JL. 1995. Regional ecosystem comparison using a standardized NDVI approach. In: Ninth annual symposium on geographic information systems. Vancouver (Canada). p 797–804.

Vitousek PM, Mooney HA, Lubchenco J, Melillo JM. 1997. Human domination of earth's ecosystems. Science 277: 494–9.

Walsh SJ, Moody A, Allen TR, Brown DG. 1997. Scale dependence of NDVI and its relationship to mountainous terrain. In: Quatrocchi DA, Goodchild MF, editors. Scale in remote sensing and GIS. Boca Raton (FL): Lewis. p 27–56.